Human Movement Science 32 (2013) 21–47

Contents lists available at SciVerse ScienceDirect

Human Movement Science

journal homepage: www.elsevier.com/locate/humov

Small perturbations in a finger-tapping task reveal inherent nonlinearities of the underlying error correction mechanism

M. Luz Bavassi [a,1], Enzo Tagliazucchi [a,1], Rodrigo Laje [a,b,c,*]

[a] Departamento de Ciencia y Tecnología, Universidad Nacional de Quilmes, R.S. Peña 352, Bernal B1876BXD, Argentina
[b] Department of Neurobiology, University of California, Los Angeles, Box 951761, CA 90095, USA
[c] CONICET, Av. Rivadavia 1917, C1033AAJ CABA, Argentina

ARTICLE INFO

Article history:
Available online 30 January 2013

Keywords:
Synchronization
Tapping
Error correction
Modeling
Dynamical systems analysis

ABSTRACT

Time processing in the few hundred milliseconds range is involved in the human skill of sensorimotor synchronization, like playing music in an ensemble or finger tapping to an external beat. In finger tapping, a mechanistic explanation in biologically plausible terms of how the brain achieves synchronization is still missing despite considerable research. In this work we show that nonlinear effects are important for the recovery of synchronization following a perturbation (a step change in stimulus period), even for perturbation magnitudes smaller than 10% of the period, which is well below the amount of perturbation needed to evoke other nonlinear effects like saturation. We build a nonlinear mathematical model for the error correction mechanism and test its predictions, and further propose a framework that allows us to unify the description of the three common types of perturbations. While previous authors have used two different model mechanisms for fitting different perturbation types, or have fitted different parameter value sets for different perturbation magnitudes, we propose the first unified description of the behavior following all perturbation types and magnitudes as the dynamical response of a compound model with fixed terms and a single set of parameter values.

* Corresponding author at: Departamento de Ciencia y Tecnologiá, Universidad Nacional de Quilmes, R.S. Peña 352, Bernal B1876BXD, Argentina. Tel.: +54 1143657100; fax: +54 1143657132.
E-mail address: rlaje@unq.edu.ar (R. Laje).
[1] Current address: Departamento de Física, Universidad de Buenos Aires, Pabellón I Ciudad Universitaria, Buenos Aires C1428EHA, Argentina.

0167-9457/$ - see front matter © 2012 Elsevier B.V. All rights reserved.
http://dx.doi.org/10.1016/j.humov.2012.06.002

1. Introduction

Time perception and production in the range of several hundreds of milliseconds, known as millisecond timing, is crucial for motor control, speech generation and recognition, playing music and dancing, and rapid sequencing of cognitive operations such as updating working memory (Buhusi & Meck, 2005; Meck, 2005). However, our understanding of the basic mechanisms underlying these behaviors is poor, and the representation of temporal information in the brain remains one of the most elusive concepts in neurobiology (Ivry & Spencer, 2004), particularly in this timing range. To date no strong consensus has been reached about which brain regions are involved in time measurement of short intervals and how they interact (Beudel, Renken, Leenders, & de Jong, 2009; Del Olmo, Cheeran, Koch, & Rothwell, 2008; Lewis & Miall, 2003; Manto & Bastian, 2007), or which is the neural mechanism responsible for the production of timed responses in this range (Buonomano & Laje, 2010). This stands in stark contrast to our rather comprehensive knowledge about temporal processing in other ranges, for example circadian timing (Panda, Hogenesch, & Kay, 2002).

1.1. Sensorimotor synchronization

A paradigmatic aspect of millisecond timing is sensorimotor synchronization, which is the ability to entrain movement to an external metronome. Although a recent study reported this ability in a variety of non-human species (Schachner, Brady, Pepperberg, & Hauser, 2009), animals display a very limited form of the behavior. In contrast, it is quite easy for humans to achieve synchronization with a metronome or musical beat and this forms the basis of all music and dance. One of the simplest tasks to study sensorimotor synchronization is finger tapping. In this task a subject is instructed to tap in synchrony with a periodic sequence of brief tones, and the time difference between each response and its corresponding stimulus is recorded (see Fig. 1). Despite its simplicity, this task helps to unveil interesting features of the underlying neural system and the error correction mechanism responsible for synchronization.

The first evidence of the existence of such a correction mechanism is the phenomenon of synchronization itself; although no single response is perfectly aligned in time with the corresponding stimulus, the responses stay in the vicinity of the corresponding stimuli throughout (see Fig. 1; note the commonly observed tendency of anticipation, called Negative Mean Asynchrony or NMA). Without a correction mechanism, tiny synchronization errors or small differences between the interstimulus interval and the interresponse interval would rapidly accumulate and make the responses drift away from the stimuli, as it is very unlikely that the subject could set his/her interresponse interval exactly at the right value—even on average. This is most evident when the subject is instructed to keep tapping at the same pace after the metronome has been muted, what is called a continuation paradigm. The "virtual asynchronies" computed between the continuing taps and the extrapolated silent beats usually get quite large within a few taps (Repp, 2005), even for musically trained subjects. Note that this crude evidence for a correction mechanism does not indicate the kind of mechanism used, since average synchronization could be achieved through either continuous adjustments (i.e., at every step), or intermittent control (i.e., once every few steps), or some other correction strategy (Gross et al., 2002), or even a mix of short- and long-range processes (Wagenmakers, Farrell, & Ratcliff, 2004).

1.2. Models for finger tapping

The behavior of the neural mechanisms underlying finger tapping synchronization is usually interpreted in terms of an error-correction function f that takes past events as inputs (including asynchronies, intervals, and interval differences) and estimates the timing of the next response. This approach assumes that the underlying mechanism can be separated into a deterministic part (the correction function itself) and noise (due to inherent variability of time estimation, motor action, etc., see the seminal paper on clock and motor variance by Wing & Kristofferson (1973)). The form of the error correction function can then be generally stated as:

$$e_{n+1} = f(e_n, t_n, r_n, T_n, \ldots) + \text{noise} \quad (1)$$

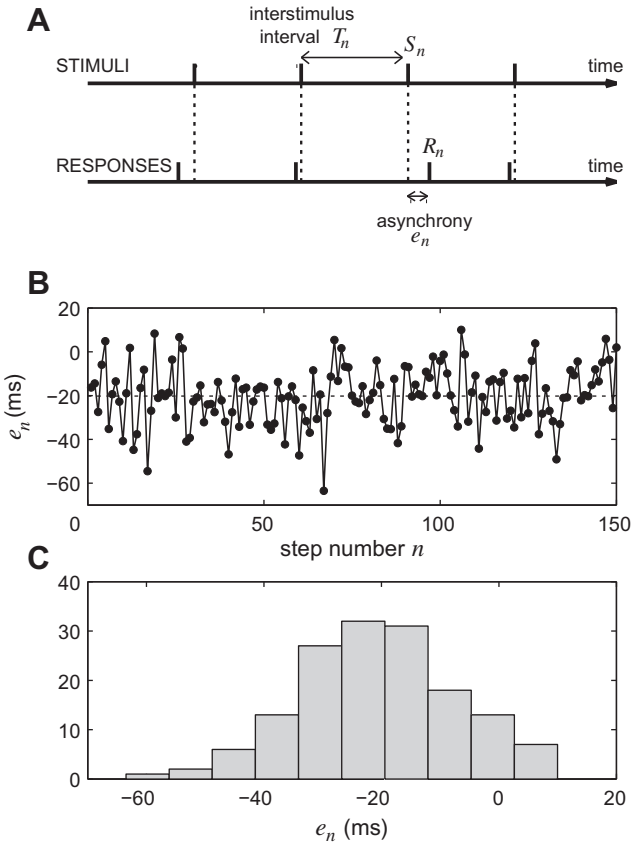

Fig. 1. The finger-tapping task. (A) Definition of variables. The subject is instructed to tap in synchrony with a metronome, and the differences $e_n = R_n - S_n$ between each tap occurrence R_n and the corresponding stimulus occurrence S_n are recorded. T_n is the interstimulus interval, and e_n is called the synchronization error or asynchrony. (B) Typical time series and (C) histogram of the synchronization error e_n for an isochronous sequence (constant interstimulus interval of 500 ms; one trial from one subject). Note the tendency to anticipate the taps (called negative mean asynchrony, NMA, depicted as a dashed line around −20 ms). The subject is normally unaware of his/her own NMA.

where e_n is the synchrony error at step n, T_n is the interstimulus interval, and r_n is the interresponse interval; the function f could have a dependency on earlier steps as well ($n-1$, $n-2$, etc.). The variable t_n is usually associated with the period of a presumed internal timekeeper (Wing & Kristofferson, 1973), as in Mates' influential dual-process error correction model for sensorimotor synchronization (Mates, 1994a, 1994b). In the dual-process model the subject is capable of adjusting the phase and period of the internal timekeeper. The error correction function is usually chosen to be linear, but nonlinear terms may be needed to accommodate saturation effects observed in perturbation experiments with large perturbation magnitudes up to 50% of the stimulus period (Repp, 2002b) or following spontaneous large synchrony errors (Engbert, Krampe, Kurths, & Kliegl, 2002). The noise term in Eq. (1) may have a complicated structure of its own (e.g., Vorberg & Schulze, 2002), and experimental data obtained with isochronous sequences can display long-range correlations (known as $1/f$ noise; Chen, Ding, & Kelso, 1997; Wagenmakers et al., 2004).

Related work within the internal timekeeper framework can be traced as far back as the pioneering work by Michon (1967), who proposed a linear predictive model that estimates the next interresponse interval based on the preceding two interstimulus intervals. Hary and Moore (1987a) proposed the

influential hypothesis that the subject estimates the timing of the next tap based randomly on either the preceding stimulus occurrence S_n or the preceding tap R_n, a strategy called "mixed phase resetting" that was later shown to be equivalent to the (now usual) assumption that the estimation is based on the synchrony error e_n (Schulze, 1992). It is still under debate which perceptual information is used by the error correction mechanism; Schulze, Cordes, and Vorberg (2005) proposed an alternative to Mates' model in which the internal timekeeper period is updated by the preceding synchrony error e_n, instead of the difference between the preceding interstimulus interval and timekeeper period, as Mates (1994a) has proposed. Even considering only one source of perceptual information, Pressing and Jolley-Rogers (1997) showed that the subject's response to an isochronous sequence can depend on the last error e_n or the last two errors e_n and e_{n-1}, depending on whether the sequence is slow or fast, and accordingly proposed a second-order autoregressive model (Pressing, 1998; Pressing & Jolley-Rogers, 1997).

An alternative theoretical framework to explain the coordination of a subject's response with a periodic sequence is based on the concepts of self-sustained attentional oscillation, phase entrainment, and period adaptation (Large, 2000; Large & Jones, 1999). It assumes that the external rhythmic signal evokes intrinsic neural attentional oscillations that entrain to the periodicities of the sequence (Loehr, Large, & Palmer, 2011), a process that can be represented by a sine circle map—a nonlinear system that can show more complex entrainments than 1:1 synchronization, such as 2:1, etc. Although oscillator and timekeeper models seem very different at first sight, linear timekeeper models can be seen as simplifications of nonlinear oscillator models and actually yield similar predictions for certain types of behavior (Loehr et al., 2011). Oscillator models probably surpass timekeeper models when stimuli with multiple periodicities are considered (Loehr et al., 2011); to the best of our knowledge, however, the extent to which they accurately reproduce the transient behavior when abrupt perturbations are considered has yet to be demonstrated—the perturbations considered by Loehr et al. (2011) were not abrupt step changes but slow linear increases or decreases in tempo, which in fact can be seen as quasi-stationary if the model is in a high dissipation regime.

1.3. Nonlinear behavior

There is evidence of nonlinearity in finger tapping tasks. Repp (2002b) and Repp (2011a) showed that the response to a phase-shift perturbation displays at least two distinctive nonlinear features: asymmetry and saturation in the phase correction response (PCR, equal to the difference between the time of occurrence of the first tap after the perturbation and the expected time when this tap would have occurred in the absence of perturbation). Asymmetry was evident as smaller values of the PCR for negative than for positive shifts, but only for perturbation magnitudes greater than ±10% of a 500 ms period (±50 ms). Saturation effects, displayed as a shallower increase of the PCR function with the size of large perturbations than of small perturbations, were also evident. Interestingly, Repp (2002b) also found an asymmetry in the standard deviation of the PCR: the variability was higher for positive than for negative perturbations, but again only outside the range ±50 ms. The asymmetric behavior of the PCR led the author to the interpretation that it is easier to delay than to advance a tap in response to a perturbation (Repp, 2011a).

So far, asymmetries have been largely reported for phase shifts only, and particularly for large perturbation sizes or asynchronies. It is remarkable that these findings have not yet been reflected in substantial changes to the linear models, despite the common observation that the estimates for the linear parameters depend for instance on perturbation magnitude (see below). To our knowledge, nonlinear models within the internal timekeeper framework have only been proposed to account for saturation of the response and only in an isochronous task. Engbert et al. (2002) proposed a nonlinear model to explain a small subset of the data in an isochronous finger tapping task. They showed that an error correction model with a saturating function $\tanh(e_n)$ was consistent with the experimental results, and interpreted it as a saturation in the subject's response when the synchrony error e_n is large.

The nonlinear behavior, however, seems pretty robust, and sooner or later the models will have to address it (Repp, 2011a). Up to now, the linear approximation appeared to be valid for small perturbation sizes. However, in this work we demonstrate asymmetric responses to step-change perturbations for perturbation magnitudes smaller than 10% of a 500 ms period, and accordingly propose a nonlinear

(quadratic) model. There is an important *qualitative difference* between a quadratic and a linear model—after symmetric perturbations, a linear model can only yield symmetric responses, showing an overshoot either to both perturbations or to none (Loehr et al., 2011). This difference cannot be addressed quantitatively with a better fitting of a linear model, and calls for a revision of the validity of linear models within the usual range of small perturbation magnitudes.

1.4. Different proposed mechanisms for different conditions

Perturbation experiments are usually performed to probe the response of the system, most notably in the form of either a "step change", or a "phase shift", or an "event-onset shift" (see Fig. 2), where both the magnitude of the perturbation and the time of occurrence are unexpected. A surprisingly common approach in the field—regardless of the chosen framework, whether timekeeper- or oscillator-based—is to fit the model's parameter values separately to different conditions, thus yielding different parameter estimates for different perturbation types and even for different perturbation magnitudes within the same perturbation type (see, e.g., Thaut, Miller, & Schauer, 1998; Repp, 2001b; Schulze et al., 2005; Large, Fink, & Kelso, 2002—for a recent exception to this common choice, see Loehr et al., 2011). Although the parameter names are the same within each model, after separate fitting the coefficient of the phase or period correction may be small for some perturbations and large for other perturbations, effectively changing the model's correction strategy and thus the interpretation

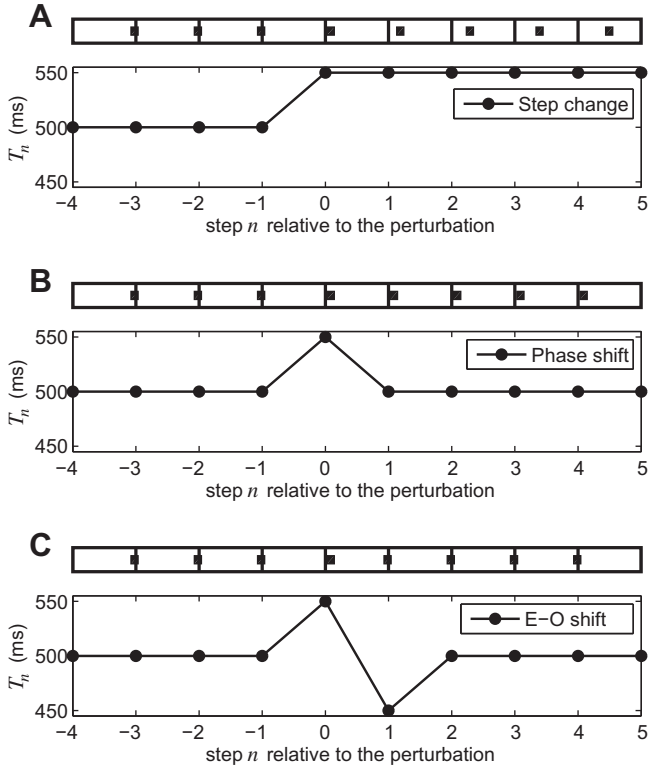

Fig. 2. The three basic perturbation types. Interstimulus interval T_n as a function of position in the sequence, relative to the perturbation ($n = 0$). (A) Step change: a single change in the interstimulus interval; it is considered the elementary perturbation in this work. (B) Phase shift: constant temporal shift of all tones following the perturbation, achieved by two consecutive elementary step changes. (C) Event-onset shift: shift of a single event, achieved by three consecutive elementary step changes. Top inset in every panel shows the corresponding tone onset times (solid squares) versus the non-perturbed period (thin vertical lines). After Repp (2005).

of the data. For instance, a study that explicitly suggested separate strategies for correcting large and small step-change perturbations is that of Thaut et al. (1998). The authors found a significant difference in their model's fitted parameter values for large and small step-change perturbations, including a huge difference of two orders of magnitude between the extreme values of the fitted β (period correction), ranging from -0.496 to -0.006, effectively making the proposed period correction term disappear for some perturbation magnitudes. This, together with the observation of apparently qualitatively and quantitatively different time evolutions for the experimental series, led the authors to state, "the observed multiple synchronization strategies are expressed in our brief mathematical model through adjustments in the equation constants".

Within the dual-process model (Mates, 1994a, 1994b), the proposed period correction process was shown to be dependent on the subject's awareness of a tempo perturbation. Repp (2001b) and Repp and Keller (2004) fitted the model separately to each perturbation size and found a significant difference between the values of the period correction coefficient β contingent on the detection responses. Awareness of the perturbation is undoubtely an important factor of the underlying mechanism responsible for the synchronization behavior. However, the subject is still able to achieve synchronization whether being aware or not. Thus, the fact that a linear compound model (period + phase correction) can reproduce the observed behavior only after separate fitting to different perturbation size conditions leaves the door open for attempting to construct a single nonlinear model that can uniformly account for the data of all conditions, as discussed in the following.

A related usual practice within the dual-process error correction framework is to consider the complete model when step-change perturbations are studied (both phase and period correction, e.g., Repp (2001b)), but only one equation for phase-shift and event-onset shift perturbations (e.g., Repp, Keller, & Jacoby, 2012). In the second condition, this is equivalent to setting all parameters of the period correction equation to zero in advance. An important shortcoming of this practice of separate fitting is that it does not offer any explanation as to how the subject would choose to "activate" the correct equation (i.e., mechanism) at the beginning of the trial, since he/she is unaware of the magnitude of the upcoming perturbation and thus it would be impossible to "shift gears" in advance. Even in the hypothetical case of the subject being able to immediately trigger the correct timing mechanism right after the first perturbed step (which is unlikely since all three types of perturbation start with the same first perturbed step, see Fig. 2), a second mechanism would be needed in addition to the usual error correction to make the choice. Therefore, the procedure of separate fitting implicitly and necessarily assumes that there should be an additional control mechanism for quickly selecting the appropriate set of parameter values, i.e., selecting different correction mechanisms or strategies described by different parameter values. Indeed, Schulze et al. (2005) estimated their model parameters separately both per tempo and tempo change condition and noted, "there must exist additional control mechanisms that determine when the period adjustment mechanism is started and stopped (e.g., by setting the period correction gain)".

A more parsimonious account of the behavior would avoid considering either different equations for different perturbations, or separate fitting, or any additional control mechanism, and instead describe the response to all perturbation types and magnitudes as the dynamical response of a fixed, possibly compound, model. As Thaut et al. (1998) posed it regarding step changes, "a self-regulatory model should be designed in which a given set of parameters in a difference equation simulates synchronization responses to step changes of all sizes [...] the ensuing model would have to be one describing a nonlinear system." Thus, some fundamental questions arise: Can we describe the behavior with a simple model and a single set of parameter values, and no additional control mechanisms? Can all these various, seemingly different observed responses be part of a broader spectrum of possible responses of a single system? Even if a two-equation model is considered (as in Mates' model), can all the various responses be correctly described without turning any of the equations off depending on the perturbation type or size?

1.5. Single model, compound mechanism

The sensorimotor synchronization behavior is likely to draw on several distinct neural processes, namely time perception, interval comparison, error detection, time production, and motor execution

(Repp, 2005). The questions posed above relate to whether this likely superposition of neural processes leads to different mechanisms for different perturbations, requiring an additional control mechanism for making the choice, or whether the whole behavior can be interpreted as the result of a compound mechanism represented by a relatively simple model with a fixed number of terms and a single set of parameter values.

In this work we search for both theoretical and experimental evidence supporting the hypothesis of a single underlying compound mechanism for the sensorimotor synchronization behavior in humans. By this we mean that, although several distinct neural processes are probably involved as we pointed out above, the error-correction mechanism resulting from the interplay of such processes can be interpreted as a single entity, as opposed for instance to separate mechanisms for correcting perturbations of different types or magnitudes. Based on the dynamical constraints that the observed behavior imposes on the possible models, we propose a mathematical model for the error correction function f (Eq. (1)), without assuming the existence of an internal clock of any particular kind, or any other hypothesis about the actual neural mechanism in charge of achieving average synchronization. We search for a unified formal framework in which the model accounts for average data from the three most common types of perturbation experiments and for all studied perturbation magnitudes with a single set of parameter values and a fixed number of equations and terms. Although not a proof, the success of such a unification effort would be suggestive evidence for the nonlinearity and the existence of an underlying compound mechanism.

2. Theoretical results

2.1. General considerations

We choose the observable synchronization error e_n as our main variable because of its fundamental nature (Chen et al., 1997), and propose an error correction model in the form of a map like Eq. (1)—that is, we propose the shape of the function f. We assume as our working hypotheses that it is possible to identify a deterministic component within the general mechanism of error correction (i.e., we assume the usual separation between a deterministic rule and noise), and that the qualitative behavior of the deterministic component can be described in terms of a small number of variables (i.e., we are not proposing a realistic neural model, but a phenomenological behavioral model). This separation between a deterministic component and inherent noise is particularly important when studying perturbations, where the deterministic rule is likely to have more importance than in an isochronous setting (which is the usual setting for studying the noise component).

One of the most influential models for the error correction mechanism (Mates, 1994a, 1994b) included motor and perceptual delays, and a distinction between external (observable) and internal (psychological/neural) variables. At this point we do not assume anything about the psychological or neural basis of the mechanism, and instead search for the dynamical constraints that the observed behavior sets on the possible models for the underlying mechanism.

2.2. Theoretical implications of previous experimental studies

Several dynamical constraints on the possible models for the underlying error-correction mechanism become evident after careful reviewing of the literature on finger-tapping tasks. In the following we pinpoint the most important findings and interpret them theoretically in order to build our model.

2.2.1. Thresholds are not needed

Perturbations to the stimulus sequence in an otherwise isochronous finger-tapping task are very informative for probing the mechanism of synchronization. One of the most common perturbations is a constant shift of all tones from a certain point in the sequence, called a "phase shift". Indeed, phase-shift perturbations were used to show that even subliminal changes smaller than 4% of the stimulus period (the approximate threshold for perceptual detection of interval changes in musicians) led to a correction behavior (Repp, 2000). Repp showed that in all cases, irrespective of perturbation

magnitude or sign, the correction mechanism was engaged already at the first tap after the (unexpected) perturbation, and the return to the baseline was monotonic (see Fig. 3A).

Although recent work (Repp, 2011a) has shown an asymmetric response to positive and negative phase shifts, and has confirmed a nonlinear response for large perturbation magnitudes (Repp, 2002b), it is clear that the qualitative shape of the time evolution of the response (averaged across trials to reduce noise) is always a monotonic recovery of synchronization, at least within the range of perturbation magnitudes studied here. In addition, error correction is engaged even at the smallest perturbation magnitude studied—smaller than the lowest achievable perceptual detection thresholds for auditory-auditory or auditory-kinesthetic temporal order (about 20 ms; Hirsh, 1959; Hirsh & Sherrick, 1961; Repp, 2000), or phase-shifts (at least 10 ms; Repp, 2000), or interval perturbations (about 4% for time intervals; Drake & Botte, 1993; about 2% for tempo changes; McAuley & Kidd, 1998; see Repp, 2000 for more references). Several other studies have also shown that subjects respond to subliminal perturbations (Hary & Moore, 1987b; Madison & Merker, 2004). This suggests that the processes

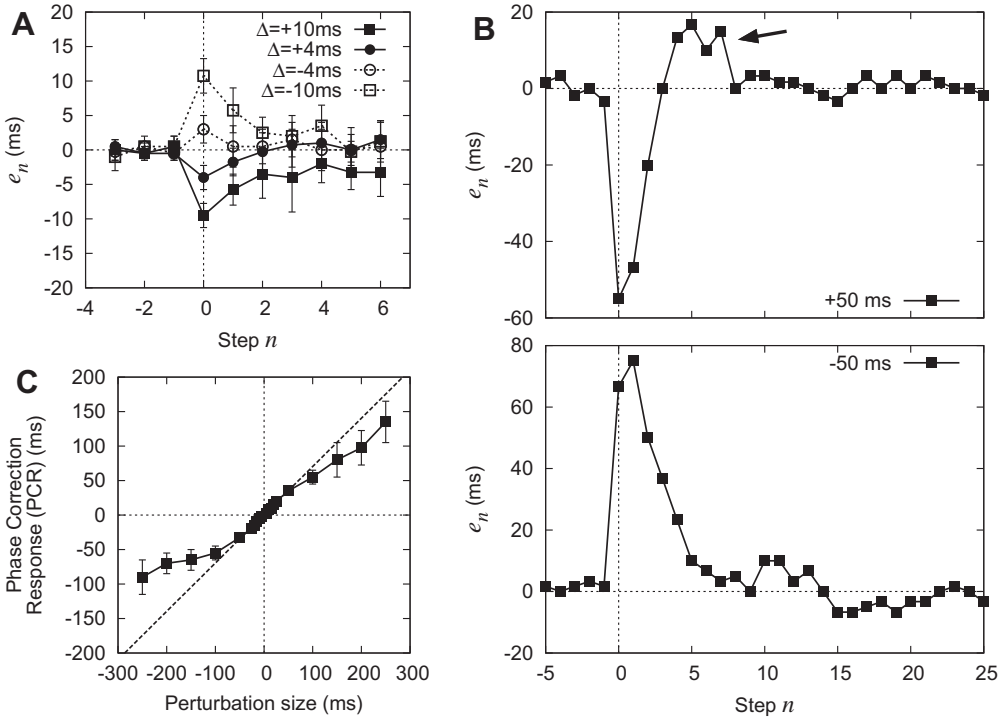

Fig. 3. Review of some published experimental results. (A) Phase-shift perturbations to a sequence with 500 ms pre-perturbation interstimulus interval. The error at step $n = 0$ is a forced error, since the perturbation is unexpected and thus the subject is unaware of how large the perturbation will be and when it will occur. Error correction is engaged already at the first step after the perturbation ($n = 1$). The overall time evolution is a monotonic return to the baseline; the qualitative shape of the time evolution is not evidently dependent on the magnitude or the sign of the perturbation. Perturbations of ±10 ms are near the detection threshold, while ±4 ms are subliminal. Data digitized and re-plotted from Repp (2000) with permission. (B) Step-change perturbations to a sequence with 500 ms pre-perturbation interstimulus interval (*top*, $\Delta = +50$ ms; *bottom*, $\Delta = -50$ ms). Error correction is evident at the first step after the forced error. There is an asymmetric response to the perturbation: the return to the baseline is monotonic after the negative perturbation, but there is an overshoot (arrow in top panel) after the positive perturbation. Data digitized and re-plotted from Thaut et al. (1998) with permission. (C) Phase correction response (PCR), or relative shift of the tap immediately following a phase-shift perturbation as a function of its magnitude, with a pre-perturbation interstimulus interval of 500 ms. The central portion of the function is linear (diagonal dashed line), but the slope decreases for larger perturbations. This could be interpreted as a saturation effect in the subject's ability to correct the asynchrony after a perturbation of large magnitude. Data digitized and re-plotted from Repp (2002b) with permission.

involved in sensorimotor synchronization have access to more accurate timing information than conscious processes of temporal judgment (Repp, 2000). An alternative, more parsimonious interpretation is based on the hypothesis that the subject times his/her next tap, in part, with reference to the shifted tone and, in part, with reference to the previous tap (Repp, 2002a; Repp, 2005), although this interpretation has been called into question by recent results (Repp, 2011b). In any case, these results imply that there is no need to incorporate detection thresholds into the models.

2.2.2. Isochronous sequences and dimensionality

Even the synchronization to an isochronous sequence (i.e., a periodic sequence without perturbations) can show nontrivial features. In such studies, the period of the sequence is varied among trials, with values typically between 200 and 750 ms (although shorter and longer periods have also been tested). Two independent studies (Pressing & Jolley-Rogers, 1997; Semjen, Schulze, & Vorberg, 2000) have shown that the correction mechanism is fed by the last synchronization error e_n for slow sequences, but by the last two synchronization errors e_n and e_{n-1} for fast sequences. That is, the experimental data were best fitted by

$$e_{n+1} = \alpha e_n \tag{2}$$

for slow sequences, and by

$$e_{n+1} = \alpha e_n + \beta e_{n-1} \tag{3}$$

for fast sequences. Pressing and Jolley-Rogers (1997) interpreted this result based on a number of observations, most notably that the fastest periods are less than or of the order of typical estimates for decision-based error correction times (Gibbs, 1965). Some degree of overlap between the processing of consecutive perceptual information is then expected in this condition. A different, plausible interpretation is based on hierarchical metrical structure, with the beat moving to a higher (i.e., slower) level for faster sequences (Repp, 2008).

We model this result as follows. Assume that the correction function is linear, at least for non-perturbed sequences. We choose to represent our system with a two-variable model fed by only the last step, instead of a single-variable model fed by the last two steps. This is possible because there is a correspondence between the two representations; a simple algebraic manipulation leads to the following identification:

$$\begin{pmatrix} e_{n+1} \\ x_{n+1} \end{pmatrix} = \begin{pmatrix} a & b \\ c & d \end{pmatrix} \begin{pmatrix} e_n \\ x_n \end{pmatrix} \Rightarrow e_{n+1} = Ae_n + Be_{n-1} \tag{4}$$

for appropriately chosen parameter values $\mathbf{M} = (a,b;c,d)$ such that $\mathrm{tr}(\mathbf{M}) = A$ and $\det(\mathbf{M}) = -B$. Here the variable x_n is an auxiliary variable of dynamical origin and in principle is not intended to represent any particular biological/neural/perceptual/physical entity (see Section 5). We interpret the crossover between slow and fast sequences (Eqs. (2) and (3)) as a reduction in the effective dimensionality of the 2D system, since setting $A \neq 0$ and $B = 0$ in the 1D system is equivalent to setting $\mathrm{tr}(\mathbf{M}) \neq 0$ and $\det(\mathbf{M}) = 0$ in the 2D system, which can be achieved by setting one of the eigenvalues to a value much smaller than the other. Indeed, if $\lambda_2 \ll \lambda_1$ then $\mathrm{tr}(\mathbf{M}) = \lambda_1 + \lambda_2 \approx \lambda_1$ and $\det(\mathbf{M}) = \lambda_1\lambda_2 \ll \lambda_1$.

We have two main reasons to choose a 2D representation (left-hand side of implication in Eq. (4)) instead of a 1D, two-step model (right-hand side of implication in Eq. (4)). First, note that the correspondence described by Eq. (4) is strictly valid for linear models only—it breaks down as soon as we include a nonlinear term. This is due to the fact that the algebraic manipulation needed to switch between the two sides involves solving for some of the variables, i.e., finding an inverse function; and the inverse of a function is not always a well-defined function when nonlinear terms are included (for instance the inverse of $z_n = e_n^2$ would be the multivalued curve $e_n = \pm\sqrt{z_n}$). Second, our choice allows us to use the tools of Nonlinear Dynamics theory and the powerful, geometrical interpretation of the phase space, which is is particularly helpful to model the two significant features we point out: overshoot and asymmetry.

2.2.3. Perturbations and dimensionality

A second common perturbation used in finger tapping experiments is a sudden increase or decrease in the period of an otherwise isochronous sequence, what is called a "step change". An interesting finding is evident in the experimental time series displayed in Fig. 3B: the asynchronies in response to a step change (here, 10% of the stimulus period of 500 ms) exhibit considerable overshoot before approaching the new baseline (Thaut et al., 1998). The overshoot after a perturbation cannot be reproduced by a one-dimensional map fed by only the last step (such as Eq. (2)), since that would violate the deterministic nature of the equation—no value of the variable can have two different possible futures (Schöner, 2002). The only behavior that such a model could display after a perturbation is either a monotonic decay to the baseline value or a monotonic divergence from it (or a constant value, if it is initially set at its asymptotic value), whatever nonlinear terms it may have. In order to reproduce an overshoot, a two-dimensional (2D) map is needed instead—or alternatively a 1D model with a two-step dependence (left and right sides of Eq. (4), respectively). As before, we choose a 2D representation.

2.2.4. Asymmetry

Another interesting finding from the step-change perturbations is that the overshoot is only displayed for positive perturbations, i.e., when the period of the sequence is increased but not when it is decreased (Thaut et al., 1998). The asymmetric behavior is a most important feature regarding the building of our model, and can be readily observed in the time series in Fig. 3B: symmetric negative and positive step-change perturbations (i.e., having equal absolute magnitudes) have an asymmetric effect on the system's response. After a step decrease in the interstimulus interval (a negative perturbation) the subject monotonically approaches the synchronization error baseline, but after a step increase (a positive perturbation) the baseline is only approached after overshooting. This asymmetry cannot be reproduced by a linear model, as discussed in the Introduction. It can be argued that the asymmetry is evidence of two distinct underlying mechanisms, or two fundamentally different ways of perturbing the system (see Section 5); we assume, however, that the asymmetric behavior is inherent to a single underlying system, and thus incorporate it in the model by introducing appropriate nonlinear terms to break the symmetry displayed by the linear part. Any even-order term (i.e., quadratic, forth-, sixth-, etc. order) would play a qualitatively similar role regarding the asymmetry; parsimoniously, we choose the lowest even order which is quadratic.

Note that the asymmetry discussed above appears after a step-change perturbation of $\Delta = \pm 50$ ms (±10%), that is just within the usual range where linear behavior is assumed (i.e., where all linear models are used). The described asymmetry could be related to the observed asymmetry in the detection threshold for step changes (Repp, 2001b), although a causal relationship between the two is not readily evident. Repp (2011a) also reported asymmetries, but in response to phase-shift perturbations and for perturbation magnitudes greater than ±75 ms (with a pre-perturbation interstimulus interval of 500 ms).

2.2.5. Saturation effects

Finally, when the perturbations are large (up to 50% of the basal interstimulus interval), saturation effects appear, at least in response to phase-shift and event-onset shift perturbations. Repp (2002b) applied phase shifts of variable magnitude and both signs to the stimuli sequence and recorded the relative shift of the tap immediately following the perturbation (that is, the PCR). He found that the amount of correction was a linear function of the perturbation magnitude for small perturbations (between 10% and −10% of the initial stimulus period), but the slope of the function decreased for larger perturbations, giving the PCR function a sigmoid-like shape possibly reflecting a saturation in the correction ability (see Fig. 3C; and also Repp, 2011a). Engbert et al. (2002) found evidence of saturation effects in isochronous sequences. They tested the synchronization time series for unstable periodic orbits and rejected the null hypothesis of an underlying linear system in about 4% of the series in the experimental dataset. Engbert et al. (2002) assumed that the subject's ability for correcting deviations is different for small and large deviations—a common, biologically plausible assumption—and modeled this saturation effect by adopting a correction function of a sigmoid shape (tanh). This implies an asymptote that would probably be only evident in the extreme case, if any, of a very large

perturbation, as the ±50% ones in Repp (2002b). For smaller perturbation magnitudes, the same effect is seen as a decreasing slope in the PCR function. In a low-order modeling approach as ours, the existence of an asymptote or saturation would not be represented by a full tanh function, but by its next-to-linear term in the Taylor series, which is a cubic term (consideration of even larger perturbation sizes would probably need the inclusion of a fifth-order term, etc.). Since we focus on small perturbations (10% or less) to limit the amount of nonlinear phenomena in the data, for the sake of simplicity—and to avoid the likely masking of the smaller, second-order effects—we choose to disregard saturation effects and thus we do not incorporate such nonlinearity into our model.

We thus propose a model with linear and quadratic terms. From a dynamical systems perspective, there is a clear-cut ranking for simplicity: what is the order of the highest-order term in the model? In this sense, a quadratic model is the next-to-simplest model. On the other hand, a function like tanh for instance (usually representing saturation) can be very compact but in fact it can be considered as a placeholder for an infinite sum of terms with any desired odd power ($\tanh(x) \sim x + a\ x^3 + b\ x^5 + c\ x^7 + \cdots$).

2.3. Model equations

According to our previous considerations, we propose the following two-dimensional model for the correction function in a finger tapping task:

$$\begin{aligned} e_{n+1} &= a e_n + b(x_n - T_n) + \alpha e_n (x_n - T_n) + \beta (x_n - T_n)^2 \\ x_{n+1} &= c e_n + d(x_n - T_n) + x_n \end{aligned} \tag{5}$$

where e_n is the (observable) synchronization error, or asynchrony, at step n; x_n is an auxiliary variable of dynamical origin, not intended in principle to represent any biological/neural/perceptual/physical entity but necessary to reproduce the overshoot and the 2D behavior described above; T_n is the interstimulus interval at step n, entering as a parameter; a,b,c,d are the linear coefficients; and α,β are the coefficients of the nonlinear terms, needed to reproduce the asymmetric response to step-change perturbations.

The linear part of the model superficially resembles that of other (linear) two-dimensional models, such as those of Mates (1994a) and Schulze et al. (2005). Note, however, that the timekeeper period equation in Mates' model does not depend on the asynchrony e_n, and in Schulze and colleagues' model it only depends on the asynchrony e_n. We propose, instead, the most general linear part: the two variables are coupled to each other (i.e., both variables appear linearly in both equations) with arbitrary linear coefficients. This choice has the following rationale: our aim is to encompass all three perturbation types within the same description, and thus at this point we choose not to remove any term in the linear part in order to get the most general behavior from the model in the vicinity of the fixed point. The fitting of the model to the experimental data will tell us whether any linear coefficient should be zero or not.

The proposed nonlinear terms, as argued in Section 2, must be quadratic for the model to reproduce the observed asymmetric behavior described in Section 2.2.4. Note that the most general set of quadratic terms has the following six terms (disregarding the parameter T_n for simplicity): $\alpha e_n x_n + \beta x_n^2 + \gamma e_n^2$ in the first equation and similarly $\theta e_n x_n + \kappa x_n^2 + \phi e_n^2$ in the second equation. We obtained acceptable fitting to the experimental data (described below) by using quadratic terms in only one of the equations; furthermore, using any two terms would yield similar results, but only one term seemed to be insufficient. Much work is needed to unveil the role of each nonlinear term, such as finding and modeling bifurcations like those leading to the influential model of Haken, Kelso, and Bunz (1985) for bimanual coordination.

It is easy to see that for isochronous sequences, where $T_n = T$ for all n, this model has a fixed point at $e_n = 0$ and $x_n = T$. The values for the linear coefficients should be such that the fixed point is stable—that is, the asynchrony e_n tends to zero and x_n tends to the value of the constant interstimulus interval T—, and in particular a stable node (in dynamical systems' terminology, we discarded other possible stable solutions like stable spirals because the experimental data does not show any consistent oscillation while approaching synchrony, and stars and degenerate nodes because of the need for carefully tuning

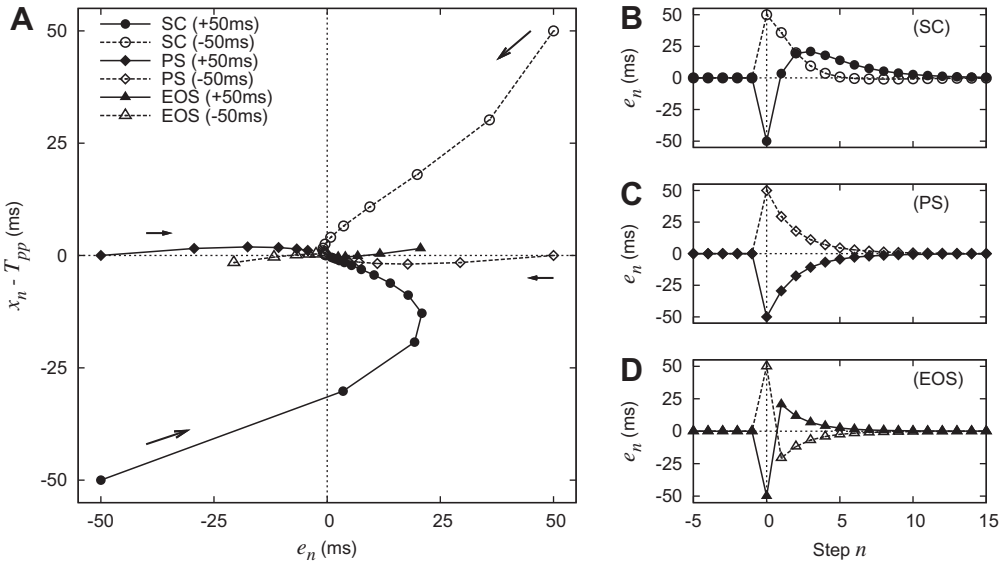

Fig. 4. Model trajectories in phase space (A) and corresponding time series (B–D) (Eq. (5)). Six conditions are displayed: step changes (SC), phase shifts (PS), and event-onset shifts (EOS), each with two possible magnitudes $\Delta = \pm 50$ ms. (A) Phase space. The trajectories are attracted to the stable fixed point (the point of subjective synchrony) after perturbing at $n = 0$ an otherwise isochronous sequence with interstimulus interval $T = 500$ ms. For visual clarity, only the portion of the trajectory after perturbation is plotted ($n \geqslant 0$ for SC and PS; $n \geqslant 1$ for EOS). (B) Step change: note that significant asymmetry in the time series only occurs in this perturbation. (C) Phase shift: synchrony is recovered after mostly symmetric, monotonic approach to baseline. (D) Event-onset shift: note the "switched" behavior: the positive (negative) perturbations are corrected from above (below). All perturbations: T_{pp} stands for "post-perturbation interstimulus interval", $T_{pp} = T + \Delta$ (for SC), $T_{pp} = T$ (for PS and EOS). Parameter values are displayed in Table 1.

the parameters—the linear coefficients should be set such that the two eigenvalues are exactly equal). For a view of the most relevant trajectories in our model's phase space, see Fig. 4. The set of parameter values used throughout this work is displayed in Table 1.

Note that we do not account for the constant NMA generally displayed by the subjects, because the target of our modeling effort is how the system responds to perturbations—the transient, not the equilibrium—, and so we shift the pre-perturbation baseline (the point of subjective synchrony) to zero by simply setting $e_n \rightarrow e_n - \text{NMA}$ (see Section 3). Other authors have extended their models such that they accommodate nonzero mean asynchronies without explaining them (Schulze et al., 2005; Thaut et al., 1998), or have included terms representing generic perceptual delays that effectively work as free parameters to accommodate a constant shift (Semjen, Vorberg, & Schulze, 1998). These models, including our own model, do not rest on a detailed description of the processing mechanisms of sensory information—they propose a phenomenological approach to the error correction function, due to the multitude of neural substrates likely involved. Few of these models account for the NMA; none of them accounts for it with a single set of parameter values; none of them accounts for it under

Table 1
Model parameter values used throughout this work. Linear coefficients a–d are nondimensional and nonlinear coefficients have units of 1/time, such that all terms in Eq. (5) have units of time. T is the pre-perturbation interstimulus interval.

$a = 0.588$	$\alpha = -0.0021\ \text{ms}^{-1}$
$b = -0.264$	$\beta = 0.0099\ \text{ms}^{-1}$
$c = -0.031$	$T = 500$ ms
$d = -0.365$	

perturbations; and none of them account for the pre-post perturbation shift in NMA as a function of the perturbation size (which is a novel finding described below). In fact, the only mathematical models that can address the NMA in synchronization tapping—without actually modeling the details of the processing mechanisms—are coupled oscillator models or circle maps (Large, 2000; Loehr et al., 2011), where the NMA arises as the stationary phase difference between the oscillatory attentional focus ("forced oscillator") and the periodic metronome ("forcing stimulus").

2.3.1. Perturbations in the model

An essential feature of our model is how it responds to perturbations. First, we assume that the interstimulus interval enters the model as a parameter T_n, and thus we interpret a step-change perturbation as a single step change in the value of T_n at step $n = 0$ (see Fig. 2A):

$$\begin{aligned} T_n &= T \quad (n < 0) \\ T_n &= T + \Delta \quad (n \geqslant 0) \end{aligned} \tag{6}$$

Second, a phase-shift perturbation in this framework is not an elementary perturbation but is formed by two consecutive step changes. The interstimulus interval changes twice such that it remains the same after the perturbation ($T \rightarrow T + \Delta \rightarrow T$), and the net effect is a time shift of all subsequent events (see Fig. 2B). Finally, an event-onset shift perturbation is composed of three consecutive step changes, and the final interstimulus interval is the same ($T \rightarrow T + \Delta \rightarrow T - \Delta \rightarrow T$, Fig. 2C).

All perturbations considered in this work are assumed to be unexpected, meaning that the subject knows that a perturbation is possible but does not know whether it will actually occur, or the time, or its magnitude or its sign. As the subject is unaware, this results in a forced error at the first step of the perturbation, on average equal to the magnitude of the perturbation (with opposite sign). We can conceptualize this by unfolding the variable e_n into "predicted e_n" and "actually observed e_n" (the difference being, on average, equal to the perturbation size at the step when a perturbation occurred, or zero otherwise). In a step-change perturbation experiment, the predicted e_n and the actually observed e_n are both zero until the perturbation arrives of size Δ. At the perturbation step the predicted e_n is still zero (because the perturbation is unexpected), but the actually observed e_n will be $-\Delta$ (on average). So, in order to let the model "know" that a perturbation occurred at step n, the parameter T_n should be changed to the new value $T + \Delta$ *and* the value of the variable e_n should be reset and overridden by the value of "actually observed e_n", that is $-\Delta$. If the variable e_n at the perturbation step has a value that is different from zero because of previous history, then the value of "actually observed e_n" is the opposite of the perturbation size $-\Delta$ plus the current e_n (with the corresponding sign), as it naturally occurs in the experiment.

Thus, in this model, any time the sequence is perturbed the variable e_n should be reset as described above to reproduce the forced error, which has the effect of resetting the initial conditions of the subsequent evolution (see Fig. 4). For a sequence with original period T that is perturbed by Δ at step $n = 0$, and assuming that the asynchrony before the perturbation was zero, the correct way to represent a step-change perturbation in the model is then

$$\begin{aligned} T_0 &= T + \Delta \\ e_0 &= -\Delta \end{aligned} \tag{7}$$

with $T_{n>0} = T + \Delta$ and subsequent evolution of e_n for $n > 0$ given by the model's equations.

2.4. Model predictions for step-change perturbations

The geometrical organization of the trajectories in our model's phase space (Fig. 5A) allows us to make a prediction about the overshoot after a step-change perturbation. Note in Fig. 5A that the approach to the fixed point after a positive perturbation (i.e., from below) always displays an overshoot in e_n, and the amount of overshoot depends on the perturbation magnitude. On the other hand, the overshoot is almost undetectable for negative perturbations (i.e., from above), regardless of the perturbation magnitude. A possible alternative hypothesis, not supported by our model, is that the

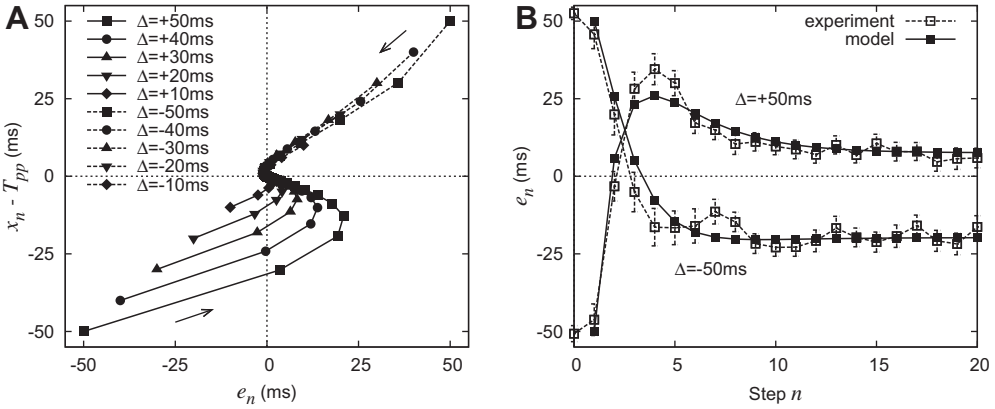

Fig. 5. Model prediction for step-change perturbations. (A) Model trajectories after a step-change perturbation of variable magnitude (Δ = ±50, ± 40, ± 30, ± 20, and ±10 ms). Note the organization of the trajectories after the perturbation, particularly the overshoot in e_n after positive perturbations (i.e., from below): a prediction of our model is that the amount of overshoot would increase with the perturbation magnitude, while negative perturbations would not display overshoot. Parameter values are displayed in Table 1. (B) Fitting of the model to our experimental data (see Section 3). Experimental data: mean across subjects ± standard error of the mean. The model was fitted using the ± 50 ms step-change perturbations only (shown here; the complete dataset is shown in Fig. 6A and D).

overshoot only appears after a large positive perturbation of 50 ms (as displayed by the experimental data in Fig. 3B) and not for smaller perturbation magnitudes.

We tested our model's prediction by performing a finger-tapping experiment with step-change perturbations. The published data for step-change perturbations deal with short trials and perturbation magnitudes of only up to 5% (Repp, 2001b), or longer trials and larger magnitudes but a limited number of intermediate magnitudes (Thaut et al., 1998). Since we needed long trials in order to let the subject reach the equilibrium possibly after an overshoot, and the behavior for intermediate perturbation magnitudes was important to test the predictions of the model, we performed our own experiment with 60-tone trials and step-change perturbations of ±50, ± 40, ± 30, ± 20, and ±10 ms (that is, between ±10% and ±2%, see Section 3). The model was fitted with a genetic algorithm to the ±50 ms time series only (Fig. 5B), i.e., only the extreme perturbations, which were the only ones used for the building of the model. The rationale behind this choice is that all intermediate perturbations would serve as a test for the model's predictions.

3. Materials and methods

3.1. Participants

The experiment consisted of a finger-tapping task with step-change perturbations. The participants were 10 volunteers (one female, ages 18–36), with no previous training in finger-tapping tasks. Most participants had substantial musical training (7 years or more; only two had less than 3 years). Five of them played percussion.

3.2. Materials and equipment

The recording of finger tapping with a standard keyboard and computer has a number of drawbacks, such as delays due to multitasking operating systems, delays due to the keyboard buffer, the key elastic response to tapping, full key depression versus key oscillation, etc. To overcome these difficulties we designed and built an electronic transducer which communicates both ways with a desktop computer through a stereo full-duplex sound card sampling at 8 kHz, yielding a time resolution of

0.125 ms (for either the presentation of the stimuli or the recording of the responses). Participants tapped using a small electrode attached to their finger's tip on a rigid ground copper plate (the subjects were electrically isolated). The small electrode was connected through a resistor to a 9 V battery, so that the electronic transducer detected the tap by the change in electrode voltage. The voltage drop triggered an LM555 timer operating in monostable mode which produced a standardized square pulse of 50 ms duration; the pulse is then registered as a sound signal in one channel of the sound card. Sound feedback from the tap was produced by a second LM555 in astable mode (600 Hz) using the output of the first timer as the envelope. The stimulus was represented by a similar logic signal that was played as a sound file through the sound card. The transducer then transformed the logic signal into an audible bip by operating a similar tandem of LM555 timers in monostable (sound envelope) and astable (sound oscillation) modes, generating pulses of 320 Hz frequency and 50 ms total duration. The envelope of the stimulus signal was registered simultaneously on the second channel of the sound card so that any delay either in the recording software or the operating system or the electronic transducer affected equally both channels, leaving the asynchronies unaltered. The delays produced by the electronic processing in the transducer were measured and found to be smaller than 50 μs. Recording and playback of logic signals through the sound card were performed using Audacity 1.2.6, which is a free, open-source software for recording and editing sounds. The data were analyzed using custom code in MATLAB. Printed-circuit board and a detailed list of components are available from the authors on request.

We chose to use auditory feedback from the taps in order to reduce timing variability (Drewing & Aschersleben, 2003), which was important to show the subtle asymmetry effect in the smaller perturbation magnitudes, and to have a more realistic musical context, as our modeling effort was meant to be relevant for musical contexts and interpersonal synchronization. The presence of auditory feedback is a difference between our work and some of the previous research (e.g., Repp, 2001b; Repp, 2002a).

3.3. Procedure and data

Participants listened over headphones at a comfortable intensity and tapped with their index finger on the copper plate. Each trial consisted of a sequence of 60 tones (pre-perturbation interstimulus interval 500 ms) and was perturbed only once, randomly between the 20th and the 30th tone. There were 5 perturbation magnitudes (10, 20, 30, 40, and 50 ms) and 2 perturbation directions (positive and negative). Each tempo change was presented 5 times. Each participant was presented with 50 sequences (5 magnitudes $\times$ 2 directions $\times$ 5 repetitions) in random order. Participants were instructed to synchronize their taps with tones as accurately as possible. They were alerted that the tone sequence might change tempo at a random position. After each trial, they were asked to report if they were aware of any perturbation.

We recorded the absolute times of occurrence of every tone (S_n) and tap (R_n) as described above, and took the differences $e_n = R_n - S_n$. For each condition (perturbation magnitude $\times$ direction) we aligned the data at $n = 0$ and averaged within subjects, then averaged across subjects. All experimental data shown represent mean across subjects ± standard error. To exclude irrelevant variation due to interindividual differences in the pre-perturbation baseline, we computed the pre-perturbation baseline as the average of the ten asynchronies before the perturbation ($-9 \leqslant n \leqslant 0$) for each condition and then subtracted this value from all asynchronies in the corresponding time series, such that the pre-perturbation baseline was close to zero.

3.4. Post-perturbation baseline

We observed a systematic shift of the baseline (presumably representing the point of subjective synchrony) from before to after the perturbation. This is a novel result discussed below, and was quantified by taking the average of the last 10 asynchronies of the corresponding experimental time series for each condition and subject (after relativizing to the corresponding pre-perturbation baseline as described above), and then averaging across subjects.

3.5. Genetic algorithm and model simulations

The fitting of the model was performed by a genetic algorithm in C, using both custom-written code and the GAUL libraries (http://www.gaul.sourceforge.net). Numerical simulations were performed with custom code in C. Code files are available from the authors on request.

The choice of a genetic algorithm was based on the following reasoning. It is known that the system to be optimized, if nonlinear, could undergo a bifurcation after the fitting algorithm changes the value of any parameter, which could be reflected in a discontinuity in the fitness function. This is an important shortcoming of gradient-based algorithms, as all gradient algorithms are ill-defined for non-differentiable objective functions. Additionally, gradient descent and methods like Newton or Gauss-Newton by their own definitions can only find the closest local optimum, a particularly important shortcoming when dealing with a nonlinear model in a 6-dimensional parameter space like ours.

On the other hand, genetic algorithms first perform an efficient search across the entire parameter space (as defined by the initial parameter ranges), find a good global solution, and then find the local optimum around it. While it is true that sometimes a genetic algorithm can converge to a local optimum (as many methods do, other than brute force exhaustive search), this can be avoided by several "countermeasures" like for instance just increasing the mutation rate, or performing the evolution several times and then choosing the absolute optimum (the chosen strategy in our case).

The six model parameters were arranged into one chromosome with six genes, and were initialized randomly with a uniform distribution in the ranges $-1.0 < a,b,c,d < 1.0$ and $-0.01 < \alpha,\beta < 0.01$, which almost exhausts the possible combinations of meaningful values (larger values for the linear coefficients for instance would mean that the variable e_n be corrected by a proportion greater than 100% of the previous value; also, large values would most likely yield eigenvalues greater than 1, with the unrealistic result that the time series would be repelled away from the point of subjective synchrony).

The fitness function was defined as minus the square root of the average squared deviation between model series and experimental series at each step. That is, if the experimental time series is E_n^j and the model time series is e_n^j ($n = 1,\ldots,20$ is the step number, $j = 1,2$ represents the two conditions ±50 ms used to fit the model), then the fitness function F reads

$$F = -\sqrt{\frac{1}{40}\sum_{j=1}^{2}\sum_{n=1}^{20} w_n^j \left(E_n^j - e_n^j\right)^2 + P}$$

which decreases as the differences $E_n^j - e_n^j$ get larger in absolute value. The weights w_n^j were chosen to counteract the effect of the shallower, longer approach to equilibrium and give more importance to the quicker, shorter transient part right after the perturbation:

	$w_n^{j=1}$	$w_n^{j=2}$
$1 \leqslant n \leqslant 3$	20	2
$4 \leqslant n \leqslant 8$	30	20
$9 \leqslant n \leqslant 20$	1	1

In order to prevent survival of unrealistic solutions (for instance damped oscillations, as discussed in Section 2.3), penalties were included as a positive term P inside the square root that depends on the linear coefficients only and takes a large value in any of the following cases:

1. The eigenvalues are complex (in order to avoid oscillatory approach to the equilibrium);
2. The eigenvalues are real but any of them is either greater than 1 or negative (in order to avoid solutions that diverge from the equilibrium, and convergent solutions that alternate sides);
3. The eigendirections have slopes with same sign, or the absolute value of any slope is less than 10° or greater than 80° (in order to enforce a generic approach to the equilibrium from each side).

The algorithm was stopped at 50 generations, which allowed the fitness function to reach a constant value. Crossover rate and mutation rate were set at the usual values of 0.9 and 0.1, respectively, and the population size was 500. In order to prevent the selection of a surviving local optimum, the whole procedure described so far was repeated 100 times; the chosen solution was the one with the highest fitness of all ($F = -14.8$). Subsequent analysis of the set of 100 partial solutions revealed a unimodal distribution for every parameter estimate, building confidence on the global nature of the chosen solution. The converged linear coefficients are of the same order as previously published values (see for instance Repp, 2001a; Thaut et al., 1998; Schulze et al., 2005).

The model was fitted to the time series data from our step-change perturbation experiment, using the $\Delta = \pm 50$ ms time series only (i.e., only the extreme perturbations). Note that ±50 ms were the only step-change perturbation magnitudes considered in the building of the model. In this way, the response to all intermediate perturbation sizes would be a test for the model's predictions. To improve fitting, a constant baseline was added to the model variable e_n after the simulated perturbation, with a fixed value equal to the experimental post-perturbation baseline of the corresponding perturbation size. For reasons discussed below, we fitted our model to the experimental time series for steps $n \geqslant 1$.

3.6. Amount of overshoot δ

The amount of overshoot δ, which is a function of the perturbation size, was defined for the positive perturbations as the difference between the maximum of the time series and the post-perturbation baseline for each condition; the error is the error of the maximum (zero in the case of the model). For negative perturbations, the amount of overshoot δ was defined likewise but using the minimum of the time series instead. Note that this definition, although very straightforward, is also very crude and can yield a value of δ different from zero even if there is no overshoot, provided that the time series are noisy. To see this, consider a finger tapping experiment to an isochronous metronome with no perturbations—since the time series is naturally noisy, the difference between the maximum (or the minimum) and the average value will obviously always be different from zero despite being a stationary time series (i.e., no overshoot at all).

In order to compensate for this bias, we applied to the experimental overshoot estimates a simple correction based on the variability of the data (the model time series had no noise, and so the overshoot estimates for the model did not need any correction). For positive perturbations, after finding the maximum as described above, the standard error of the corresponding post-perturbation baseline data was subtracted from the maximum; analogously for negative perturbations, the standard error was added to the minimum. Still, the following inconsistency could appear: in an isochronous sequence (or a sequence with a very small perturbation magnitude), the overshoot estimate after correcting could be negative if detected from above but positive if detected from below. In order to avoid this inconsistency and match both sides at zero perturbation, if an estimate of an overshoot (either maximum or minimum) changed sign after correcting, it was set to zero.

4. Experimental results

4.1. Step-change perturbations

Our experimental time series are displayed in Fig. 6, along with simulations of our model using the parameter values fitted in Fig. 5B (see Table 1 and Section 3).

The qualitative agreement between data and model is remarkable, particularly because all simulations were performed with a single set of parameter values and because the model was fitted to the ±50 ms perturbations only. The response to positive perturbations (top row) displays an overshoot which is larger for larger perturbation magnitudes, while for the negative perturbations (bottom row) the overshoot is almost undetectable, both features as predicted by our model.

There are quantitative differences worth noticing, though, which can be seen in the right column of Fig. 6. While the overshoot is well reproduced at the two largest perturbations ($\Delta = +50$ and +40 ms, compare panels A and B), in the experimental data it appears to develop more slowly for smaller

perturbations which is evidenced in panel C by a larger difference at steps $n = 1$ through $n = 5$ (see the awareness data below). The largest discrepancies occur around step $n = 2$ for both positive and negative perturbations.

Related to this observation, note in panels A and D that the empirical data show little change between steps $n = 0$ and $n = 1$ for all perturbation sizes, and exactly the same behavior can be observed in the previous literature (compare with Fig. 3B). It takes one step—or perhaps two steps at the smallest magnitudes—for the subjects to fully develop their response to a step change, both for positive and negative perturbations (though it should also be noted that the correction mechanism is at least partially engaged already at $n = 1$, otherwise the time series would follow a straight line with slope $-\Delta$). Our model does not account for this feature—nor does any other published model to the best of our knowledge unless the parameter values are changed for each condition (tempo, perturbation size, etc.). A possible interpretation is that the subject is aware that a perturbation happened (note that it occurs for supraliminal perturbations) but does not immediately interpret it as a change in stimulus period; alternatively, the subject could not be able to correct completely despite being aware of the nature and size of the perturbation. The hypothesis that the neural mechanisms underlying the correction behavior do not fully unfold until at least $n = 1$ cannot be ruled out at this point. Accordingly, we fitted our model to the experimental time series for $n \geqslant 1$. A more complete description of this particular feature is under development, and further experimental manipulation will be needed to decide whether it is related to awareness or not.

The main prediction of our model is shown in Fig. 7, which displays the amount of overshoot δ as a function of the perturbation size Δ (see Section 3). Despite the quantitative differences described above between the time series, the correspondence between the amount of overshoot in the

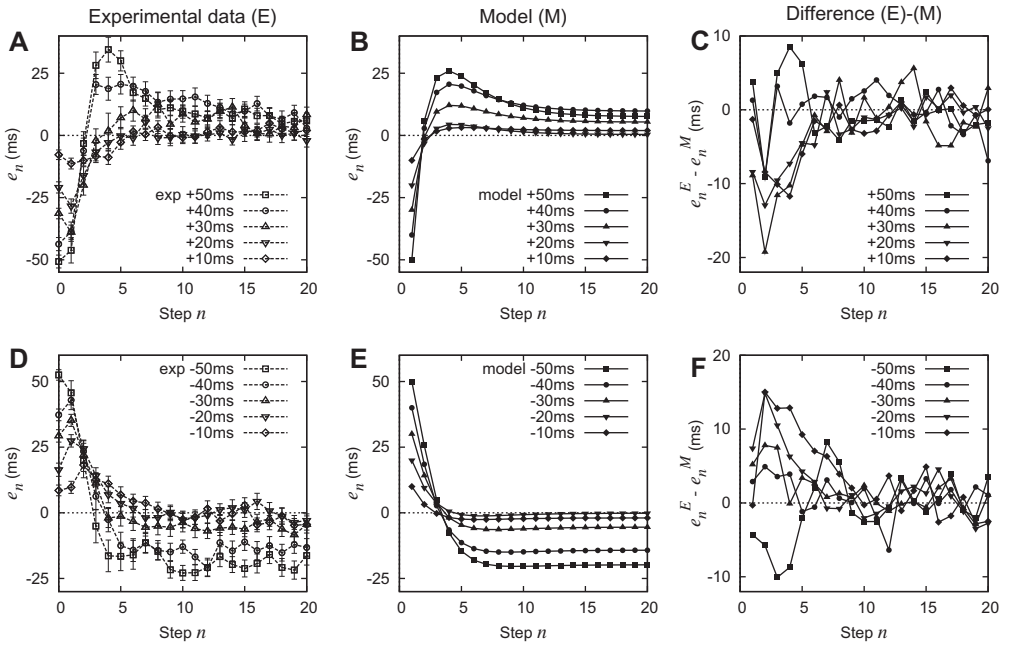

Fig. 6. Experiment and simulation of positive (*top row*) and negative (*bottom row*) step-change perturbations. (*Left column*) Experimental results from our finger tapping task (averaged responses, with standard error bars across subjects). As predicted by our model, there is increasing overshoot with increasing perturbation magnitude for positive perturbations only (panel A). (*Middle column*) Time series of the model. All model simulations throughout this work use the same set of parameter values (see Table 1). (*Right column*) Difference between the corresponding experimental (E) and model (M) time series. The difference is greater at smaller perturbation magnitudes, due to the experimental series developing the recovery more slowly than the model series.

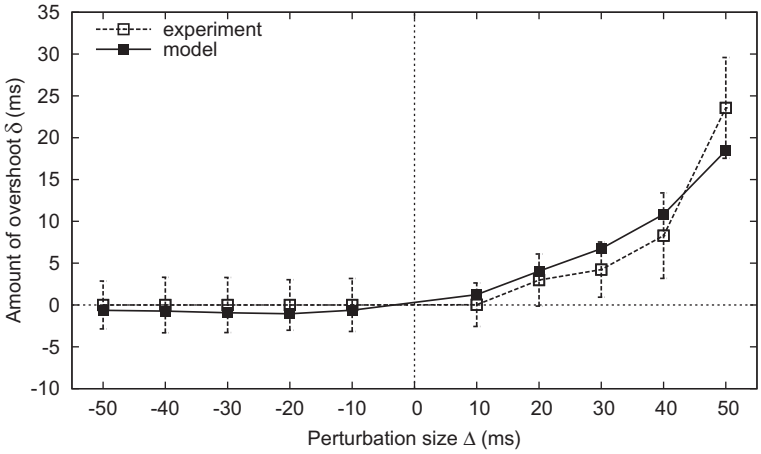

Fig. 7. Direct comparison between our model's prediction of overshoot following step-change perturbations and our experimental data. The amount of overshoot δ is zero for negative perturbations, whereas for positive perturbations it is an accelerating, increasing function of the perturbation size. Each point here was computed from the corresponding time series in Fig. 6, thus the only points coming from fitting are the two extremes $\Delta = \pm 50$ ms.

experimental data and the model simulations is remarkable (recall that the only time series used to fit the model correspond to the extreme points in this plot, $\Delta = +50$ and -50 ms). Both the experiment and the model display a very similar nonlinear relationship between overshoot δ and perturbation size Δ, with a flat profile at negative perturbations and a smooth, accelerated increase at positive perturbations.

4.2. Phase-shift and event-onset shift perturbations

Our model is also capable of reproducing the observed behavior following phase-shifts and event-onset shifts. This should be considered as a prediction too, since we did not take into account any of these two perturbations in the building of the model, except for the observation that the response to subliminal phase shifts is not limited by a threshold (Section 2.2.1). In the same line of reasoning as above for step changes, we treat phase-shift and event-onset shift perturbations as follows.

In a phase-shift perturbation, the interstimulus interval before and after the perturbation has the same value, where the main effect is the resetting of the variable $e_0 \to e_0 - \Delta$ due to the unexpected "shift" of the stimulus at $n = 0$ (Section 2.3.1). We base our modeling on the observation that the response of the subjects to a step change takes at least one step to fully develop (Section 4.1), together with the fact that in a phase shift the interstimulus interval returns to the original value after two steps (Section 2.3.1). We then assume that the only effect of this perturbation on our model is the resetting of the variable e_n at step $n = 0$ with no change in T_n. The subsequent evolution of e_n for $n \geqslant 1$ is given by the model's equations.

In an event-onset shift perturbation, the interstimulus interval returns to the original value after three steps. Consistently, we assume that the only effect on our model is the resetting of the variable in two steps, with no change in T_n. At the first step of the perturbation, $n = 0$, the variable is changed $e_0 \to e_0 - \Delta$. At the second step $n = 1$ the variable should be reset again in the opposite direction $e_1 \to e_1 + \Delta$. Notice that this does not mean that the consecutive perturbations should cancel each other, because the correction mechanism is already engaged at step $n = 1$ and thus $e_1 \neq e_0 - \Delta$. Subsequent evolution of e_n for $n \geqslant 1$ is given by the model's equations.

As can be seen in Fig. 8, the correspondence between experimental data (taken from the published literature) and our model's traces after both phase shifts and event-onset shifts is remarkable (even quantitatively). Note that the fitting of the model was performed using data from a different perturbation type (our own ±50 ms step change data).

4.3. Individual data

Fig. 9 displays the experimental time series of four subjects, averaged across repetitions, from our own data (step changes). There are some noticeable interindividual differences; for instance, subject MA displays the slowest return to the baseline, both for positive and negative perturbations. Subject PA displays the smallest range of post-perturbation baselines for positive perturbations, but the largest range for negative perturbations. The overall qualitative behavior, however, is common to all subjects.

The right column in Fig. 9 displays the amount of overshoot δ as a function of perturbation size Δ for the individual subjects. Although some subjects display a few points noticeably below zero for negative perturbations (e.g., subject RU at $\Delta = -50$ ms), all subjects share the same asymmetry—positive perturbations display larger overshoot than negative perturbations.

4.4. Shift in post-perturbation baseline and effect of awareness

Another novel finding is the systematic shift of the baseline from before to after the perturbation, shown in Fig. 10A. Note first the asymmetric dependence on the perturbation size: positive

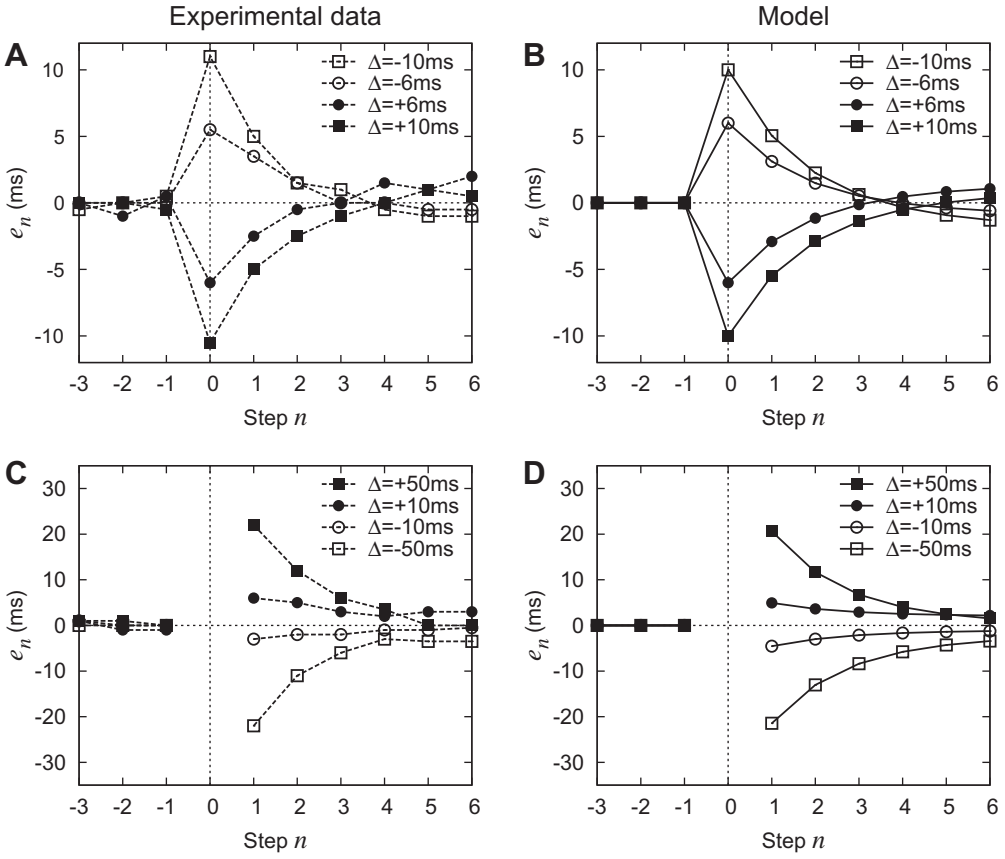

Fig. 8. Predictions for other perturbation types. Published experimental data (*left*) and numerical simulations from our model (*right*), for phase-shift (*top*) and event-onset shift (*bottom*) perturbations. The similarity is remarkable, especially because none of these perturbations were included in the building of the model or used for the fitting. All simulations in this work were performed with the same set of parameter values (Table 1). Experimental phase shifts: data digitized and re-plotted from Repp (2001a); experimental event-onset shifts: data digitized and re-plotted from Repp (2002a); all with permission.

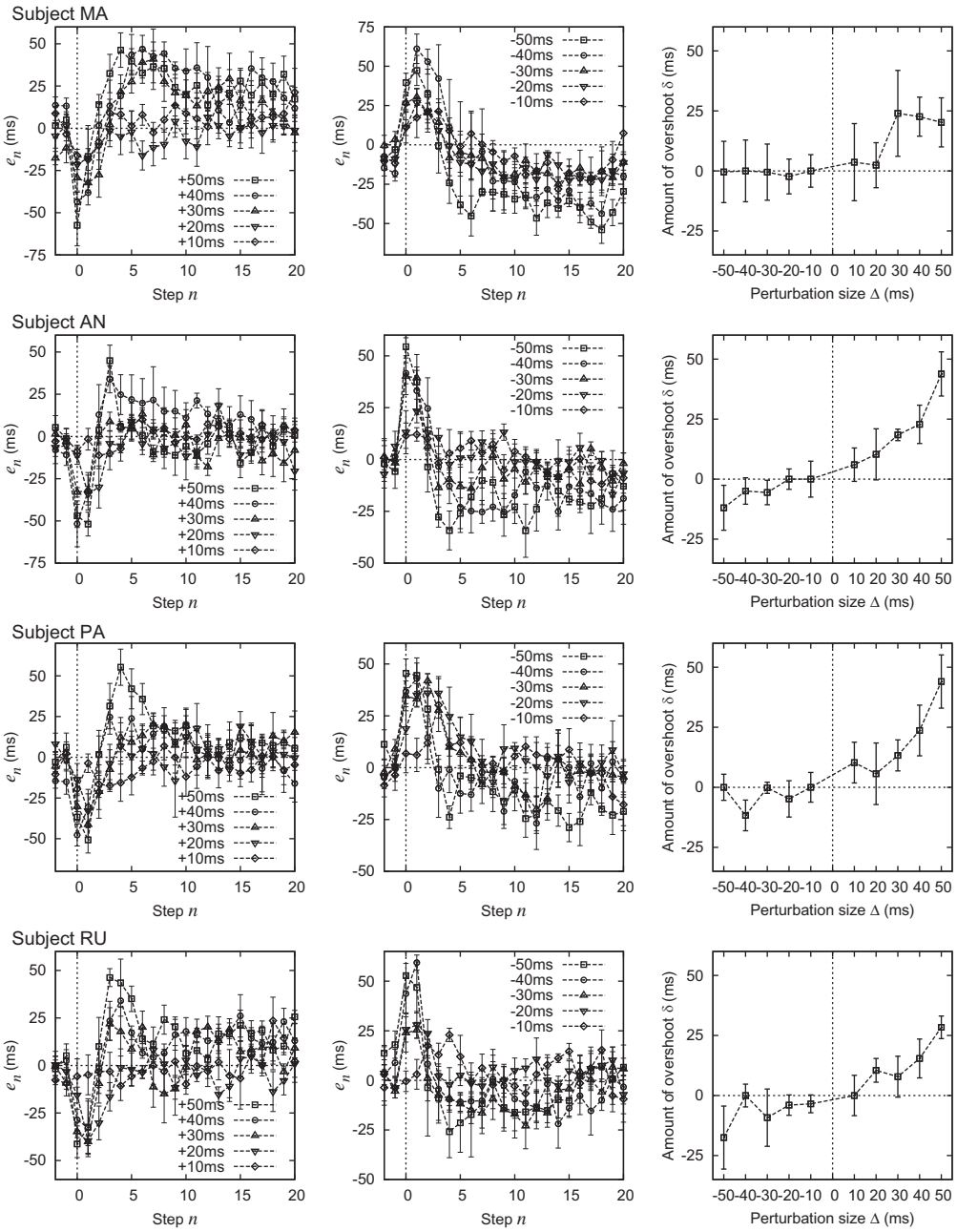

Fig. 9. Individual data from four subjects. (*Left*) Positive and (*Middle*) negative perturbations; mean of 5 trials ± standard error for each perturbation size. Despite interindividual differences (like the slower overshoot and return to baseline of subject PA), the qualitative behavior is common to all subjects: overshoot in the left column but not in the right column. (*Right*) Amount of overshoot δ. Note the greater values of overshoot for positive perturbations.

perturbations lead to smaller (in absolute value) post-perturbation baseline shifts than negative perturbations. Note also that the baseline shift in the ±20 and ±10 ms perturbations is very close to zero. The shift in pre-post baseline could also be seen in the step-change data reported by Repp (2001b,

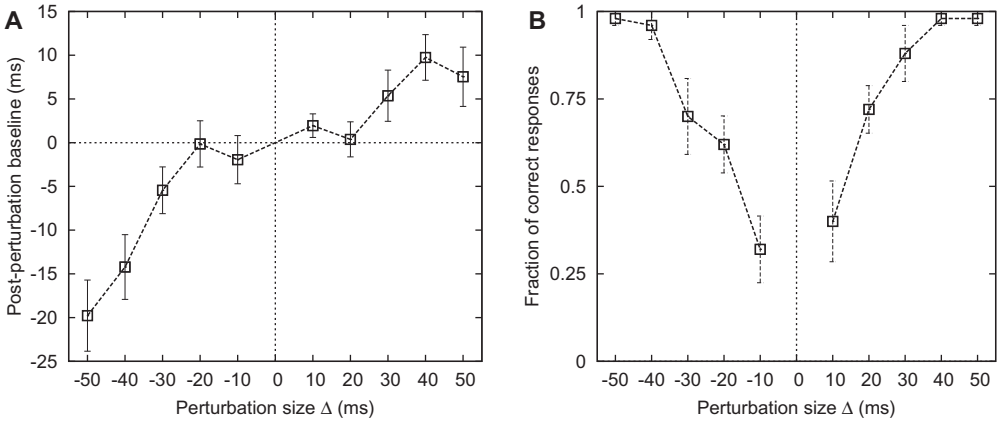

Fig. 10. (A) Post-perturbation baseline (relative to its pre-perturbation value). The baseline after a perturbation increases as a function of perturbation size (i.e., it becomes more positive for slower sequences and more negative for faster ones), which cannot be explained by the known decrease of NMA with decreasing interstimulus interval for auditory sequences. Mean across subjects ± standard error of the mean. (B) Detection of perturbations: average percentage of trials where the perturbation was detected. The ±10 ms perturbations are just below the detection threshold (0.5). Mean across subjects ± standard error of the mean.

Fig. 4), although in his data even the smallest perturbation sizes seem to display the shift. The difference is probably due to two factors (most of our subjects had extensive musical training, and we used auditory feedback from the taps) which are known to decrease the NMA (Aschersleben, 2002). Very small NMAs on both sides of the perturbation could lead to very small baseline shifts, particularly for small perturbation magnitudes. Thaut et al. (1998) also found NMA shifts after step-change perturbations to a period of 500 ms, although only for the $\Delta = \pm 20$ ms conditions (but not ±50 ms nor ±10 ms) and the shift was in the opposite direction.

Fig. 10B displays the fraction of correct responses (detection of whether a perturbation occurred or not) as a function of the perturbation size. Note that the smallest perturbations (±10 ms) were just below the detection threshold (0.5) and thus were undetectable most of the times. Even the ±20 ms perturbations were near the detection threshold, though above it. This could explain the slower development of the overshoot after the positive perturbations (Fig. 6) at the smallest perturbation magnitudes.

5. Discussion and conclusions

Although pioneering work on timing goes back as far as the 19th century, e.g., Stevens (1886), the representation of time in our brain has only recently begun to rise as a fundamental issue in neuroscience (Ivry & Schlerf, 2008). During the last decade, several studies have been published on the theoretical and experimental aspects of neural timing (Buhusi & Meck, 2005; Ivry & Schlerf, 2008; Mauk & Buonomano, 2004) and sensorimotor synchronization (for a thorough review see Repp, 2005). Still, our understanding of how the brain discriminates between two interval durations or how it produces precisely timed motor responses is far from clear.

In the case of sensorimotor synchronization, where several, probably distinct neural systems are recruited—most notably sensory and motor timing—, a behavioral approach has proven to be fruitful (Repp, 2005). This approach groups into a single model the representation of several different neural processes, namely the perception of time intervals, comparison and decision making, and the production of timed motor responses. Detailed theoretical modeling of the neural bases for time estimation in the range of hundreds of milliseconds is an active area of research, both for sensory and motor timing (for reviews see Buonomano & Laje, 2010; Ivry & Schlerf, 2008); many central issues such as whether sensory and motor timing rely on the same circuitry are unresolved. Thus, the particular features that

characterize the sensorimotor synchronization behavior—distinguishing it from either pure time perception tasks, or pure decision making tasks, or pure time production tasks—make the behavioral approach a very valuable one, at least until we reach a deeper understanding of its internal workings.

In our work we thus take a similar behavioral approach, in the spirit of searching for the dynamical constraints that the observed behavior would set on a future model of the underlying neural system. Any neural model proposed to account for the behavior should take those constraints into consideration. As an analogy, consider a system where the experimenter has only access to a stroboscopic measure of some observable, rather than to the actual continuous underlying variables—any detailed model of the underlying system should have a Poincaré section that resembles the dynamics of the stroboscopic measure.

5.1. Nonlinear behavior

We showed that the behavior consistently displays nonlinear effects in the form of an asymmetric time evolution of the response following a small step-change perturbation (smaller than 10% of the period), whereas common nonlinear effects in the PCR—which is the same for all three perturbation types—were reported at larger perturbation magnitudes: 25–50% for saturation, and $\geqslant$10% for asymmetry (Repp, 2002b, 2011a). Fig. 7 provides strong evidence of nonlinear effects, i.e., asymmetric overshoot, at small perturbation magnitudes, where the behavior is traditionally represented by linear models. It is possible that overshoot may occur also after negative step changes if larger perturbation magnitudes are considered. However, it is clear that any future model would still have to reproduce the asymmetric features shown here for smaller perturbation magnitudes.

It could be argued that the asymmetry is related to the computational costs for correcting positive and negative asynchronies (Aschersleben, 2002). The costs might differ, because correcting a step decrease in stimulus period would necessitate shortening the interresponse interval accordingly and thus carry a loss of processing time. However, this is not consistent with the experimental data shown in Fig. 6: if shortening the interresponse interval is more computationally involved, then a fast and straightforward recovery like the one occurring after a step decrease—a monotonic exponential convergence to the baseline—would not be expected. Analogously, a step increase—where the subject would have indeed more time for computational purposes—would not be expected to trigger a less accurate response like an overshoot.

Repp and Keller (2004) performed step change experiments and fitted the dual-process Mates' model (Mates, 1994a, 1994b) to the data separately for different conditions. The authors stated, "The crucial assumption of the two-process model is that phase correction and period correction are independent of each other, so that their behavioral effects are additive", and "phase correction and period correction seem to represent independent processes". The need for quadratic terms demonstrated in our work, however, speaks against strictly additive effects and calls for a revision of the idea of independent processes (particularly because of the cross-term $\propto e_n x_n$).

The interpretation of the nonlinear terms should be approached with care. Within the traditional dual-process framework (Mates, 1994a, 1994b), the internal timekeeper is updated by period and phase correction and thus a cross term like $\propto e_n\, x_n$ would be interpreted as an interaction between the two processes. This interaction could occur for instance because of shared neural substrates or crosstalk between different substrates (see for instance Praamstra, Turgeon, Hesse, Wing, & Perryer, 2003). This does not mean that an interaction between period and phase correction processes is necessary for the internal timekeeper to work well or to be precise. In fact, the experimentally observed asymmetry and overshoot can hardly be considered as "desirable" features of any proposed correction mechanism—perhaps this is just the way it is.

Within a psychological framework, where the variable e_n might be interpreted as a measure of the subject's perception of the asynchrony and the variable x_n as a measure of the subject's perception of the interstimulus interval duration (or probably the subject's estimate of the next interstimulus interval—see below), the cross term $\propto e_n x_n$ could be interpreted as an interaction between the two percepts, or also as follows. Recall Eq. (5) and note that the terms $e_{n+1} = a\, e_n + \propto e_n x_n + \ldots$ can be regrouped as $e_{n+1} = (a + \propto x_n) e_n + \cdots$. This helps interpreting the nonlinear cross term as a correction to the linear term; that is, the coefficient of e_n is not constant but varies, and its value is modified by x_n. This might

be interpreted as a tempo dependence of the correction mechanism; however, caution must be taken as x_n is only asymptotically equal to T_n (the interstimulus interval, or tempo), i.e., once synchrony is achieved. In much the same way, the term βe_n^2 can be interpreted either as an "auto-interaction" or as a correction to the coefficient of the linear term: $ae_n + \beta e_n^2 = (a + \beta e_n)e_n$. According to this interpretation, the amount of correction coming from the perception of an asynchrony would be disproportionally larger for larger asynchronies. This effect would counteract any additional saturating term (e.g., cubic) to some extent, with the effect of the higher-order term overcoming the lower-order one at large enough asynchronies or perturbation magnitudes.

Further work is needed to unveil the true meaning of the nonlinear terms. We found, for instance, some parameter interdependence: the estimates for α and β are negatively correlated (data not shown). This means that two different parameter value sets can account for the data to the same extent: either with a larger α and a smaller β (and thus with a more important interaction between the two variables), or the other way around (and thus a more important auto-interaction e_n^2). Quadratic terms, however, are necessary to reproduce the observed behavior anyway.

The systematic shift of the post-perturbation baseline with respect to its pre-perturbation value was an unexpected finding (Fig. 10A), also pointing to asymmetric features of the behavior but unexplained by our model. It is known that the NMA for auditory sequences depends on the interstimulus interval (Repp, 2003), displaying a shallow decrease spanning less than 20 ms as a function of the interstimulus interval in the range 320–680 ms (i.e., it becomes more negative for slower sequences). The NMA after the perturbation could change because the interstimulus interval changes. However, our result is not consistent with that: the post-perturbation baseline in our experiment actually increases as a function of the perturbation size (i.e., it becomes more positive for slower sequences). It seems to be dependent on awareness (because it only appears after perturbations larger than ±20 ms), but it also seems to be dependent on the perturbation size (i.e., not constant) if the perturbation is above the detection threshold. Future work should reconcile this finding with the accepted causes and explanations for the NMA, e.g., a slower central registration of tactile and proprioceptive information as compared with the auditory modality, or the phase lag in coupled oscillator models; see Repp (2005) for a review. The fact that we used auditory feedback from the taps and that most of our subjects had extensive musical training—both factors making the NMA decrease (Aschersleben, 2002) and thus the NMA shift decrease—are likely causes for the absence of a shift in the NMA at the smallest perturbations (±20 and ±10 ms).

5.2. Single model, compound mechanism

Beyond the mere fitting of a new model, we proposed a unified view for the effect of a perturbation on the behavior. This unified framework is a first step to consistently include the perturbation within the modeling effort (Thaut et al., 1998), an important goal when interpersonal or crowd synchronization is studied, as in music, or in computer-human synchronization experiments. Moreover, our model takes into account the three most common finger-tapping perturbations on an equal basis. Previous studies have fitted a different set of parameter values to each perturbation magnitude (see, e.g., Thaut et al., 1998; Repp, 2001b; Schulze et al., 2005). We emphasize that our model correctly predicts the relationship between overshoot and perturbation size for the step-change perturbations, and qualitatively predicts the evolution of the observed asynchronies following all studied perturbation types and magnitudes with a single set of parameter values, a fixed number of terms, and both equations always "turned on".

The sensorimotor synchronization behavior is likely to draw on several distinct neural processes, namely time perception, interval comparison, error detection, time production, and motor execution. However, the question remains open as to whether this superposition leads to different mechanisms or strategies for different perturbations (as proposed for instance by Thaut et al. (1998) or Schulze et al. (2005)), or whether the whole behavior can be interpreted as the result of a single compound mechanism. This second, more parsimonious account would perhaps consider a slightly more complex system with a dynamics that inherently and "automatically" reproduces the observed behavior, without turning equations off or changing the value of the parameters for different perturbation types and magnitudes. The different terms in our model might or might not correspond to different underlying

neural processes. A key issue in our proposal, however, is that we do not turn them on and off depending on the perturbation type or magnitude, or change the value of their coefficients. The two equations that constitute our model are always "on" and with constant parameter values. It is in this sense that our model points to a single compound mechanism—there are no "different strategies" given by different sets of parameter values; there is no need to "choose" between mechanisms (i.e., equations); there is no need to resort to additional mechanisms whose task would be to select the appropriate value of the parameters; and there is a fixed set of terms in the model.

The overshoot in e_n is a quite robust behavior after step increases, and can be noticed also in Fig. 4B of Repp (2001b), after removing the pronounced linear drift displayed by the subjects after the perturbation. This evidence points to the need for a two-dimensional model: as discussed in the Theoretical Results, the overshoot cannot be explained in terms of a single variable only, even if it occurred for both positive and negative step changes. We then proposed a second variable, x_n, whose evolution is given by an equation that resembles the so-called "period correction" mechanism (Repp, 2005), although it is more general. Several previous studies have proposed two distinct correction processes, namely phase and period correction mechanisms, based on the hypothesis that there is an internal timekeeper or oscillator whose parameters can be reset or modified (see for instance Mates' influential timekeeper model (Mates, 1994a, 1994b), and Large's oscillator model (Large, 2000)). Perhaps more parsimoniously, we propose that our variable x_n might be interpreted as either a measure of the subject's perception of the interstimulus interval duration or the subject's estimate of the next interstimulus interval (based on either the alleged internal oscillator or a more complex neural construct (Buonomano & Laje, 2010)). A more complex, although probably true, interpretation is that x_n is a compound measure of all. It is difficult to base interpretations on the relationship between model parameters and the underlying neural/psychological system without further experimental manipulation, particularly because of the composite nature of this behavior. Further investigation will be necessary to establish the neural/psychological identity of the dynamical variable x_n.

Phase shifts and event-onset shifts are usually regarded as more primitive and simple forms of perturbation than step changes (Repp, 2005). This could be due to the smaller perceptual impact on the subject; indeed, if no correction were made, the asynchrony after a phase shift would remain constant, and after an event-onset shift there would be no asynchrony at all, whereas the asynchrony after a step change would increase linearly with time. However, we argue for a different interpretation. Since in our framework the step change perturbation involves only one change in parameter value ($T \rightarrow T + \Delta$), while the phase shift involves two changes ($T \rightarrow T + \Delta \rightarrow T$) and the event-onset shift involves three changes ($T \rightarrow T + \Delta \rightarrow T - \Delta \rightarrow T$), we argue in favor of considering the step change a more fundamental perturbation. Our model consistently incorporates this interpretation. The remarkable result, however, is not that the model can be driven through phase shifts or event-onset shifts as a concatenation of step changes; what we find remarkable is that the experimental data from the other perturbation types are correctly predicted as a concatenation of step changes (Fig. 8). To our knowledge, it is not known whether the neural mechanisms/strategies underlying the response to a step change are the same as those underlying a phase shift or an event-onset shift. However, we succeeded in predicting both experimental phase shifts and event-onset shifts as a concatenation of responses to individual step changes, which in addition suggests that the underlying system might be considered as a single compound mechanism.

Repp and Keller (2004) demonstrated that the fits of the dual-process Mates' model (Mates, 1994a, 1994b) to data with tempo perturbations changed significantly contingent on the subject's awareness. Although our model shows a lack of a quantitative fit right after the perturbation for the smallest perturbation sizes (Fig. 6C and F; less awareness might lead to a slower/softer triggering of the response which leads to larger departures of the model from the data at the smaller perturbation magnitudes), it does offer qualitatively successful description and predictions of the behavior, which suggests that both detectable and undetectable perturbations could be accounted for quantitatively by a single model (single set of parameter values) in the future. This does not imply that awareness is not a factor of the underlying neural system; on the contrary, since the subjects are still able to achieve synchronization whether the perturbation is subliminal or not, and the experimental data do not show any qualitative difference between the two conditions, a possible interpretation is that the part of the underlying system responsible for the awareness has a response which is dependent on the size of

the perturbation, but is otherwise always "on". This could be nicely described by a model with a single set of parameter values, as opposed to a description in terms of "on" and "off" states (represented by changes in parameter values and/or terms that are removed by the experimenter). Future work should address this particular behavior, and also the response to larger perturbation magnitudes and other base tempos.

Acknowledgments

We thank Dean V. Buonomano, Mariano Sigman, Juan Kamienkowski, Manuel C. Eguía, Andrés Benavides, and Guillermo Solovey for helpful discussions and comments. We thank Bruno Repp, Nori Jacoby, and an anonymous reviewer for detailed suggestions to improve the manuscript. This work was supported by CONICET and ANPCyT PICT-2007-881 (Argentina), and the Fulbright Commission (USA-Argentina).

References

Aschersleben, G. (2002). Temporal control of movements in sensorimotor synchronization. *Brain and Cognition, 48*, 66–79.
Beudel, M., Renken, R., Leenders, K. L., & de Jong, B. M. (2009). Cerebral representations of space and time. *NeuroImage, 44*, 1032–1040.
Buhusi, C. V., & Meck, W. H. (2005). What makes us tick? Functional and neural mechanisms of interval timing. *Nature Reviews Neuroscience, 6*, 755–765.
Buonomano, D. V., & Laje, R. (2010). Population clocks: Motor timing with neural dynamics. *Trends in Cognitive Sciences, 14*, 520–527.
Chen, Y., Ding, M., & Kelso, J. A. S. (1997). Long memory processes ($1/f^{\alpha}$ type) in human coordination. *Physical Review Letters, 79*, 4501–4504.
Del Olmo, M. F., Cheeran, B., Koch, G., & Rothwell, J. C. (2008). Role of the cerebellum in externally paced rhythmic finger movements. *Journal of Neurophysiology, 98*, 145–152.
Drake, C., & Botte, M.-C. (1993). Tempo sensitivity in auditory sequences: Evidence for a multiple-look model. *Perception and Psychophysics, 54*, 277–286.
Drewing, K., & Aschersleben, G. (2003). Reduced timing variability during bimanual coupling: A role for sensory information. *The Quarterly Journal of Experimental Psychology, 56A*, 329–350.
Engbert, R., Krampe, R. T., Kurths, J., & Kliegl, R. (2002). Synchronizing movements with the metronome: Nonlinear error correction and unstable periodic orbits. *Brain and Cognition, 48*, 107–116.
Gibbs, C. B. (1965). Probability learning in step-input tracking. *British Journal of Psychology, 56*, 233–242.
Gross, J., Timmermann, L., Kujala, J., Dirks, M., Schmitz, F., Salmelin, R., et al (2002). The neural basis of intermittent motor control in humans. *Proceedings of the National Academy of Science Uniteed States of America, 99*, 2299–2302.
Haken, H., Kelso, J. A. S., & Bunz, H. (1985). A theoretical model of phase transitions in human hand movements. *Biological Cybernetics, 51*, 347–356.
Hary, D., & Moore, G. P. (1987a). Synchronizing human movement with an external clock source. *Biological Cybernetics, 56*, 305–311.
Hary, D., & Moore, G. P. (1987b). Temporal tracking and synchronization strategies. *Human Neurobiology, 4*, 73–77.
Hirsh, I. J. (1959). Auditory perception of temporal order. *Journal of the Acoustical Society of America, 31*, 759–767.
Hirsh, I. J., & Sherrick, C. E. (1961). Perceived order in different sense modalities. *Journal of Experimental Psicology, 62*, 423–432.
Ivry, R. B., & Schlerf, J. E. (2008). Dedicated and intrinsic models of time perception. *Trends in Cognitive Sciences, 12*, 273–280.
Ivry, R. B., & Spencer, R. M. C. (2004). The neural representation of time. *Current Opinion in Neurobiology, 14*, 225–232.
Large, E. W. (2000). On synchronizing movements to music. *Human Movement Science, 19*, 527–566.
Large, E. W., Fink, P., & Kelso, J. A. S. (2002). Tracking simple and complex sequences. *Psychological Research, 66*, 3–17.
Large, E. W., & Jones, M. R. (1999). The dynamics of attending: How people track time-varying events. *Psychological Review, 106*, 119–159.
Lewis, P. A., & Miall, R. C. (2003). Brain activation patterns during measurements of sub- and supra-second intervals. *Neuropsychologia, 41*, 1583–1592.
Loehr, J. D., Large, E. W., & Palmer, C. (2011). Temporal coordination and adaptation to rate change in music performance. *Journal of Experimental Psychology: Human Perception and Performance, 37*, 1292–1309.
Madison, G., & Merker, B. (2004). Human sensorimotor tracking of continuous subliminal deviations from isochrony. *Neuroscience Letters, 370*, 69–73.
Manto, M., & Bastian, A. J. (2007). Cerebellum and the deciphering of motor coding. *The Cerebellum, 6*, 3–6.
Mates, J. (1994a). A model of synchronization of motor acts to a stimulus sequence: I. Timing and error corrections. *Biological Cybernetics, 70*, 463–473.
Mates, J. (1994b). A model of synchronization of motor acts to a stimulus sequence: I. Stability analysis, error estimation and simulations. *Biological Cybernetics, 70*, 475–484.
Mauk, M. D., & Buonomano, D. V. (2004). The neural basis of temporal processing. *Annual Review of Neuroscience, 27*, 307–340.
McAuley, J. D., & Kidd, G. R. (1998). Effect of deviations from temporal expectations on tempo discrimination of isochronous tone sequences. *Journal of Experimental Psicology: Human Perception and Performance, 24*, 1786–1800.
Meck, W. H. (2005). Neuropsychology of timing and time perception. *Brain and Cognition, 58*, 1–8.
Michon, J. A. (1967). *Timing in temporal tracking*. Assen, The Netherlands: van Gorcum.

Panda, S., Hogenesch, J. B., & Kay, S. A. (2002). Circadian rhythms from flies to human. *Nature, 417*, 329–335.
Praamstra, P., Turgeon, M., Hesse, C. W., Wing, A. M., & Perryer, L. (2003). Neurophysiological correlates of error correction in sensorimotor-synchronization. *NeuroImage, 20*, 1283–1297.
Pressing, J. (1998). Error correction processes in temporal pattern production. *Journal of Mathematical Psychology, 42*, 63–101.
Pressing, J., & Jolley-Rogers, G. (1997). Spectral properties of human cognition and skill. *Biological Cybernetics, 76*, 339–347.
Repp, B. H. (2000). Compensation for subliminal timing perturbations in perceptual-motor synchronization. *Psychological Research, 63*, 106–128.
Repp, B. H. (2001a). Phase correction, phase resetting, and phase shifts after subliminal timing perturbations in sensorimotor synchronization. *Journal of Experimental Psychology: Human Perception and Performance, 27*, 600–621.
Repp, B. H. (2001b). Processes underlying adaptation to tempo changes in sensorimotor synchronization. *Human Movement Science, 20*, 277–312.
Repp, B. H. (2002a). Automaticity and voluntary control of phase correction following event onset shifts in sensorimotor synchronization. *Journal of Experimental Psychology: Human Perception and Performance, 28*, 410–430.
Repp, B. H. (2002b). Phase correction in sensorimotor synchronization: Nonlinearities in voluntary and involuntary responses to perturbations. *Human Movement Science, 21*, 1–37.
Repp, B. H. (2005). Sensorimotor synchronization: A review of the tapping literature. *Psychonomic Bulletin and Review, 12*, 969–992.
Repp, B. H. (2003). Rate limits in sensorimotor synchronization with auditory and visual sequences: The synchronization threshold and the benefits and costs of interval subdivision. *Journal of Motor Behavior, 4*, 355–370.
Repp, B. H. (2008). Multiple temporal references in sensorimotor synchronization with metrical auditory sequences. *Psychological Research, 72*, 79–98.
Repp, B. H. (2011a). Tapping in synchrony with a perturbed metronome: The phase correction response to small and large phase shifts as a function of tempo. *Journal of Motor Behavior, 43*, 213–227.
Repp, B. H. (2011b). Temporal evolution of the phase correction response in synchronization of taps with perturbed two-interval rhythms. *Experimental Brain Research, 208*, 89–101.
Repp, B. H., & Keller, P. E. (2004). Adaptation to tempo changes in sensorimotor synchronization: Effects of intention, attention, and awareness. *Quarterly Journal of Experimental Psychology, 57A*, 499–521.
Repp, B. H., Keller, P. E., & Jacoby, N. (2012). Quantifying phase correction in sensorimotor synchronization: Empirical comparison of three paradigms. *Acta Psychologica, 139*, 281–290.
Schachner, A., Brady, T. F., Pepperberg, I. M., & Hauser, M. D. (2009). Spontaneous motor entrainment to music in multiple vocal mimicking species. *Current Biology, 19*, 831–836.
Schöner, G. (2002). Timing, clocks, and dynamical systems. *Brain and Cognition, 48*, 31–51.
Schulze, H.-H. (1992). The error correction model for the tracking of a random metronome: Statistical properties and an empirical test. In F. Macar, V. Pouthas, & W. J. Friedman (Eds.), *Time, action, and cognition: Towards bridging the gap* (pp. 275–286). Dordrecht: Kluwer.
Schulze, H.-H., Cordes, A., & Vorberg, D. (2005). Keeping synchrony while tempo changes: Accelerando and ritardando. *Music Perception, 22*, 461–477.
Semjen, A., Schulze, H.-H., & Vorberg, D. (2000). Timing precision in continuation and synchronization tapping. *Psychological Research, 63*, 137–147.
Semjen, A., Vorberg, D., & Schulze, H.-H. (1998). Getting synchronized with the metronome: Comparisons between phase and period correction. *Psychological Research, 61*, 44–55.
Stevens, L. T. (1886). On the time-sens. *Mind os-XI*, 393–404.
Thaut, M. H., Miller, R. A., & Schauer, L. M. (1998). Multiple synchronization strategies in rhythmic sensorimotor tasks: phase vs period correction. *Biological Cybernetics, 79*, 241–250.
Vorberg, D., & Schulze, H.-H. (2002). Linear phase-correction in synchronization: predictions, parameter estimation, and simulations. *Journal of Mathematical Pschology, 46*, 56–87.
Wagenmakers, E.-J., Farrell, S., & Ratcliff, R. (2004). Estimation and interpretation of $1/f^{\alpha}$ noise in human cognition. *Psychonomic Bulletin & Review, 11*, 579–615.
Wing, A. M., & Kristofferson, A. B. (1973). Response delays and the timing of discrete motor responses. *Perception and Psychophysics, 14*, 5–12.